

- [2] J. Hespanha, S. Bohacek, K. Obraczka, and J. Lee, "Hybrid modeling of tcp congestion control," in *Lecture Notes in Comput. Science*, M. Di Benedetto and A. Sangiovanni-Vincentelli, Eds. Berlin, Germany: Springer, 2001, vol. 2034.
- [3] K. Johansson, H. Lygeros, and S. Sastry, H. Unbehauen, Ed., "Modeling of hybrid systems," *Encyclopedia of Life Support Syst. EOLSS*, 2004.
- [4] M. Blanke, M. Kinnaert, J. Lunze, and M. Staroswiecki, *Diagnosis and Fault-Tolerant Control*. Berlin/Heidelberg, Germany: Springer-Verlag, 2006.
- [5] H. Yang, B. Jiang, and V. Cocquempot, *Fault Tolerant Control Design for Hybrid Systems*. Berlin/Heidelberg, Germany: Springer-Verlag, 2010.
- [6] M. Babaali, M. Egerstedt, and E. W. Kamen, "A direct algebraic approach to observer design under switching measurement equations," *IEEE Trans. Autom. Control*, vol. 49, no. 11, pp. 2044–2049, Nov. 2004.
- [7] A. Alessandri, M. Baglietto, and G. Battistelli, "Receding-horizon estimation for switching discrete-time linear systems," *IEEE Trans. Autom. Control*, vol. 50, no. 11, pp. 1736–1748, 2005.
- [8] M. Baglietto, G. Battistelli, and P. Tesi, "Stabilization and tracking for switching linear systems under unknown switching sequences," *Syst. & Control Lett.*, vol. 62, pp. 11–21, 2013.
- [9] G. Battistelli, J. Hespanha, and P. Tesi, "Supervisory control of switched nonlinear systems," *Int. J. Adapt. Control and Signal Process.*, vol. 26, pp. 723–738, 2012.
- [10] R. Vidal, A. Chiuso, S. Soatto, and S. Sastry, "Observability of linear hybrid systems," in *Hybrid Syst.: Computation and Control, Lecture Notes in Comput. Sci. 2623*. Berlin, Germany: Springer, 2003.
- [11] R. Vidal, A. Chiuso, and S. Soatto, "Observability and identifiability of jump linear systems," in *Proc. 41st IEEE Conf. on Decision and Control*, Las Vegas, NV, 2002, pp. 3614–3619.
- [12] M. Babaali and M. Egerstedt, "Observability of switched linear systems," in *Hybrid Syst.: Computation and Control, Lecture Notes in Comput. Sci. 3414*. Berlin/Heidelberg, Germany: Springer-Verlag, 2004, pp. 48–63.
- [13] M. Babaali and G. J. Pappas, "Observability of switched linear systems in continuous time," in *Hybrid Syst.: Computation and Control, Lecture Notes in Comput. Sci. 3414*. Berlin/Heidelberg, Germany: Springer-Verlag, 2005.
- [14] H. Lou and R. Yang, "Conditions for distinguishability and observability of switched linear systems," *Nonlinear Anal.: Hybrid Syst.*, vol. 5, pp. 427–445, 2011.
- [15] M. Baglietto, G. Battistelli, and L. Scardovi, "Active mode observability of switching linear systems," *Automatica*, vol. 43, no. 8, pp. 1442–1449, 2007.
- [16] S. Hanba, "Further results on the uniform observability of discrete-time nonlinear systems," *IEEE Trans. Autom. Control*, vol. 55, no. 4, pp. 1034–1038, Apr. 2010.
- [17] A. Alessandri, M. Baglietto, G. Battistelli, and M. Gaggero, "Moving horizon state estimation for nonlinear systems using neural networks," *IEEE Trans. Neural Netw.*, vol. 22, no. 5, pp. 768–780, 2011.

Self-Excited Limit Cycles in an Integral-Controlled System With Backlash

Alex Esbrook, Xiaobo Tan, and Hassan K. Khalil

Abstract—In this technical note, we study the properties of self-excited limit cycles in an integral-controlled system containing a play operator. A Newton-Raphson algorithm is formulated to calculate the limit cycles, and we prove that the amplitude and period of these limit cycles have linear relationships to system parameters. These results are confirmed in simulation, where we demonstrate the ability to predict the properties of the limit cycles.

Index Terms—Backlash, closed-loop analysis, hysteresis, limit cycles.

I. INTRODUCTION

For systems with hysteresis, most existing work aims to provide sufficient conditions under which a given controller structure guarantees stability of the system in question. In particular, results in the nanopositioning literature focus on proving boundedness of the tracking error [1]–[3]. A natural question therefore is to consider the behavior of the system when these conditions are not satisfied; alternatively, what effects do hysteresis nonlinearities have on the steady-state solutions of the system? Several authors, perhaps most notably those of [4], have remarked that hysteresis can lead to unwanted oscillations. Further investigations into these oscillations are limited. One result is in [5], where conditions are presented under which the method of harmonic balance predicts the existence of periodic solutions in systems with relay hysteresis. The authors of [6] utilized the describing function method to predict the existence of a limit cycle in a Terfenol-D-based actuator, and demonstrated its existence in experiments. These works focused fundamentally on the question of existence, and did not investigate any properties of the limit cycles in detail. Describing function methods have also been used to demonstrate some approximate solutions to hysteretic systems [7], [8]. There is also some additional work on limit cycles in systems with relay hysteresis [9], which was driven primarily by researchers in the field of electronic circuits in the 60's.

In this technical note, we offer an in-depth exploration into the properties of self-excited limit cycles occurring in a particular class of systems with hysteresis. In particular, we focus on an n -dimensional linear plant controlled by an integral controller, where a play operator [10], [11] is present in the feedback loop. While the considered hysteresis model will not capture sophisticated hysteresis in systems such as smart material actuators, it has been chosen for several reasons. First, as we show in this note, it allows one to rigorously analyze the limit cycle properties and examine the impact of controller and plant parameters. Second, the results will apply directly to systems involving mechanical plays (backlashes). Finally, there are applications, such as

Manuscript received November 02, 2012; revised April 15, 2013, August 21, 2013; accepted September 03, 2013. Date of publication September 16, 2013; date of current version March 20, 2014. This work was supported by the National Science Foundation (CMMI 0824830). Recommended by Associate Editor X. Chen.

The authors are with the Department of Electrical and Computer Engineering, Michigan State University, East Lansing, MI 48824 USA (e-mail: esbrook@msu.edu; xbtan@egr.msu.edu; khalil@egr.msu.edu).

Color versions of one or more of the figures in this paper are available online at <http://ieeexplore.ieee.org>.

Digital Object Identifier 10.1109/TAC.2013.2281859

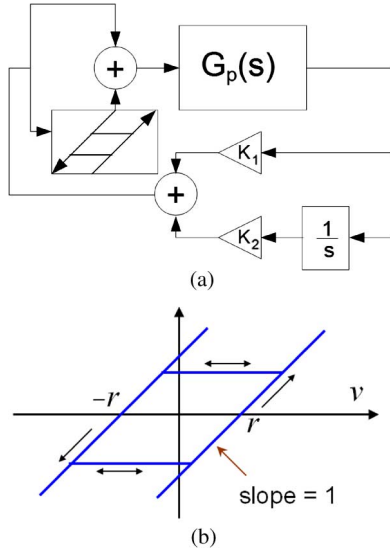


Fig. 1. (a) Closed-loop system described in (1). (b) Illustration of a play operator.

biomimetic robots, where oscillatory control inputs need to be generated [12]. The choice of a simple hysteresis model facilitates the implementation of an oscillator and offers insight as to how the oscillator output behavior (amplitude, bias, and frequency) can be tuned with the model parameters.

We focus our attention on odd symmetric limit cycles within the system. A Newton-Raphson algorithm is formulated to calculate the limit cycles, and using the odd symmetry of the operator, we are then able to prove that linear relationships exist between several properties of the limit cycles and the parameters of the system. These calculations yield precise results regarding the behavior of the limit cycles in the system, as opposed to the approximate results of the describing function method or results that focus on the question of existence. We then verify these results simulation, where we also demonstrate the effectiveness of the Newton-Raphson algorithm at predicting the solutions of the system.

A preliminary version of this note, which dealt with the case involving scalar plants only, was presented at the 2013 American Control Conference.

II. SELF-EXCITED LIMIT CYCLES IN A SYSTEM WITH HYSTERESIS

We consider a linear system preceded by a play operator and a unity gain controlled using integral control and state feedback as illustrated in Fig. 1(a);

$$\begin{aligned} \dot{x}(t) &= Ax(t) + B(v(t) + W_r[v; 0](t)) \\ \dot{\sigma}(t) &= Cx(t) \\ v(t) &= -K_1x(t) - K_2\sigma(t) \end{aligned} \quad (1)$$

where $x \in \mathbb{R}^n$, $\sigma \in \mathbb{R}$, $A \in \mathbb{R}^{n \times n}$, $B \in \mathbb{R}^n$, $C \in \mathbb{R}^{1 \times n}$, $K_1 \in \mathbb{R}^{1 \times n}$, and $K_2 \in \mathbb{R}$. The play operator W_r is a unit hysteretic element illustrated in Fig. 1(b). Each play operator W_r is parametrized by r , representing the play radius or threshold of the operator. When the input $v(t)$ is monotone and continuous, we can express the output $u(t)$ of a play operator W_r as

$$\begin{aligned} u(t) &= W_r[v; u(0)](t) \\ &= \max\{\min\{v(t) + r, u(0)\}, v(t) - r\}. \end{aligned} \quad (2)$$

The output $u(t)$ is also referred to as the state of the play operator W_r . For general inputs, the input signal is broken into monotone segments,

and the output is then calculated by setting the last output of one monotone segment as the initial condition for the next.

Notice from Fig. 1(b) and (2) that there are two basic modes in which the state of a play operator can reside. The first is the boundary region, in which $u(t) = v(t) \pm r$. The second mode of operation is the interior region, where $u(t)$ is constant, represented in (2) by the term $u(0)$. We will make use of the boundary and interior region terminology throughout the technical note. Furthermore, we will also refer to the leftmost boundary branch in Fig. 1(b) as the descending region, and the rightmost boundary branch as the ascending region. The play operator is used in the Prandtl-Ishlinskii hysteresis operator, which uses a superposition of play operators and a linear gain to model a hysteresis phenomenon [10], [11].

The well-posedness of (1) follows from the arguments in [13]. We now begin our analysis of (1) by providing a coordinate transform in order to place (1) into a switched system form. Let us define

$$\alpha(t) = -K_2\sigma(t) + W_r[v; 0](t). \quad (3)$$

The derivative of α requires us to define the derivative of a play operator, which is in general discontinuous. Let Π denote the set of all closed intervals of $t \in \mathbb{R}$ in which $W_r[v; 0](t)$ lies in a boundary region, and let Π^c denote its complement. We therefore have a piecewise continuous definition for \dot{W}_r , given by

$$\dot{W}_r[v; 0](t) = \begin{cases} \dot{v}, & \text{if } t \in \Pi \\ 0, & \text{if } t \in \Pi^c \end{cases} \quad (4)$$

where

$$\begin{aligned} \dot{v}(t) &= -K_1[(A - BK_1)x(t) + B\alpha(t)] - K_2[Cx(t)] \\ &= [-K_1(A - BK_1) - K_2C]x(t) - K_1B\alpha(t). \end{aligned} \quad (5)$$

Note that the derivative of W_r is continuous everywhere except when the play operator exits the interior region. Using (3)–(5), we can derive a switched system form for (1):

$$\begin{aligned} \dot{\gamma}(t) &= A_{i(t)}\gamma(t), \quad i = 1, 2 \\ A_1 &= \begin{bmatrix} A - BK_1 & B \\ -CK_2 & 0 \end{bmatrix} \\ A_2 &= \begin{bmatrix} A - BK_1 & B \\ -2CK_2 - K_1(A - BK_1) & -K_1B \end{bmatrix} \end{aligned} \quad (6)$$

where $\gamma = [x^T, \alpha]^T$, and r is the play radius. The matrix A_1 characterizes the systems behavior in the interior region of the hysteresis, while A_2 does so for the boundary region of the hysteresis. To describe the switching behavior of $i(t)$, we will define the operator

$$i(t) = \Omega[W_r[v; 0](t)](t) \quad (7)$$

where $\Omega[W_r[v; 0](t)] = 1$ when W_r is in the interior region, and $\Omega[W_r[v; 0](t)] = 2$ when W_r is in the boundary region. From simulations of (6) (not shown due to space limitations), we observe that if the control gains are chosen such that A_1 is unstable and A_2 is Hurwitz, the trajectories of (6) converge to a limit cycle. Furthermore, the limit cycle is sine-like, in that it is both odd-symmetric and changes the sign of its derivative twice a period. Based on these observations, we will develop a Newton-Raphson algorithm to calculate the sine-like solutions of the limit cycle.

A. Computation of the Limit Cycles

Our search for the solution of the limit cycles begins from a state γ_0 at \bar{t}_0 such that the play operator is in the ascending linear section. Let \bar{t}_1 denote the time when the play operator enters the interior region from the boundary region; this will be denoted as the first switching time. Similarly, we define \bar{t}_2 , \bar{t}_3 , and \bar{t}_4 as the second, third and fourth switching times (see Fig. 2). Since the system starts in the boundary

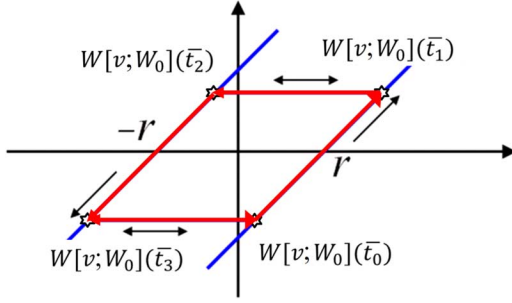


Fig. 2. Illustration of the state of the play operator P_r during a sine-like limit cycle. The stars indicate times when the system dynamics switch.

region, $i(0) = 2$, $i(\bar{t}_1^+) = 1$, $i(\bar{t}_2^+) = 2$, and so on, where \bar{t}_j^+ indicates the time moment right after \bar{t}_j , for $j = 1, 2, \dots$. Furthermore, based on our assumption of sine-like limit cycles, $\gamma(\bar{t}_4) = \gamma(0)$; therefore $\bar{t}_4 - \bar{t}_0$ is the period of the limit cycle. From the description of the play operator, for any sine-like limit cycle, the control $v(t)$ at these switching times obeys the equations

$$\dot{v}(\bar{t}_1) = 0 \quad (8)$$

$$v(\bar{t}_1) - v(\bar{t}_2) = 2r \quad (9)$$

$$\dot{v}(\bar{t}_3) = 0 \quad (10)$$

$$v(\bar{t}_3) - v(\bar{t}_4) = -2r. \quad (11)$$

Furthermore, symmetry allows us to only consider the conditions (8) and (9). We will let $t_1 = \bar{t}_1 - \bar{t}_0$ and $t_2 = \bar{t}_2 - \bar{t}_1$; these values will be referred to as the switching *intervals*. We can then translate these equations into functions of γ_0 . From (8) and the definitions of v and A_2 , we can quickly arrive at

$$H_1(\gamma_0, t_1) \triangleq \bar{K} e^{A_2 t_1} \gamma_0 = 0 \quad (12)$$

where $\bar{K} = [-K_1(A - BK_1) - K_2C, -BK_1]$. Since W_r is constant in the interior region, from (9) and (3), we can derive

$$H_2(\gamma_0, t_1, t_2) \triangleq [-K_1, 1][I - e^{A_1 t_2}]e^{A_2 t_1} \gamma_0 = 2r \quad (13)$$

where I is an appropriately dimensioned identity matrix. Finally, because we are seeking sine-like limit cycles, we also have the constraint equation

$$\Sigma^T(\gamma_0, t_1, t_2) \triangleq (I + e^{A_1 t_2} e^{A_2 t_1}) \gamma_0 = 0 \quad (14)$$

which is derived from the forward-time solution of the switched system from $t = \bar{t}_0$ to $t = \bar{t}_2$. Note that the existence of a set of values (γ, t_1, t_2) satisfying (12)–(14) will imply the existence of a sine-like limit cycle. The proof for the existence of more generally shaped limit cycles, however, is a challenge that is beyond the scope of this note. We now present the following lemma, which addresses the symmetry of the dynamics of the system.

Lemma 1: Let γ_0 be the state of (6) when the system enters the ascending branch from the interior region, and let $\gamma(\bar{t}_2)$ denote the state of (6) when it enters the descending boundary region. Assume that the system switches once between states γ_0 and $\gamma(\bar{t}_2)$. Then, if the system lies at $-\gamma_0$ at $t = \bar{t}_0$ in the descending region, the state of the system when the system enters the ascending region is $-\gamma(\bar{t}_2)$.

Proof: Based on (8) and (9), we know that γ_0 and $\gamma(\bar{t}_2)$ must obey

$$\begin{aligned} \gamma(\bar{t}_1) &= e^{A_2 t_1} \gamma_0, & \gamma(\bar{t}_2) &= e^{A_1 t_2} \gamma(\bar{t}_1) \\ 0 &= \bar{K} e^{A_2 t_1} \gamma_0 \end{aligned} \quad (15)$$

$$2r = [-K_1, 1][I - e^{A_1 t_2}] \gamma(\bar{t}_1) \quad (16)$$

where t_1 and t_2 are the switching intervals. Now consider the behavior starting from $-\gamma(0)$. Then

$$\begin{aligned} \gamma(\bar{t}_1^*) &= -e^{A_2 t_1^*} \gamma_0, & \gamma(\bar{t}_2^*) &= e^{A_1 t_2^*} \gamma(\bar{t}_1^*) \\ 0 &= -\bar{K} e^{A_2 t_1^*} \gamma_0 \end{aligned} \quad (17)$$

$$-2r = [-K_1, 1][I - e^{A_1 t_2^*}] \gamma(\bar{t}_1^*) \quad (18)$$

where \bar{t}_1^* and \bar{t}_2^* are the switching times and t_1^* and t_2^* are the switching intervals for the system when it is initialized at $-\gamma_0$. Note the minus sign on the $2r$ term in (18). This is because we are entering the opposite region of the play operator from the original case, and therefore this switching condition would be derived from (11) instead of (9). Comparing (15) with (17), we notice that the sole difference is the presence of the negative sign, which cannot affect whether $\dot{v} = 0$. Therefore, \bar{t}_1^* is equal to t_1 , implying $\gamma(\bar{t}_1^*) = -\gamma(\bar{t}_1)$. Using this in (18) yields

$$\begin{aligned} [-K_1, 1][I - e^{A_1 t_2^*}] \gamma(\bar{t}_1^*) &= -2r \\ [-K_1, 1][I - e^{A_1 t_2^*}] \gamma(\bar{t}_1) &= 2r \end{aligned}$$

Since we have recovered (16), we know that $t_2^* = t_2$, which completes the proof. \square

Remark 1: This lemma shows that as long as a γ_0 can be found such that $\gamma_0 = -\gamma(\bar{t}_2)$, the system possesses a sine-like limit cycle. However, this result is proved under the assumption that the sign of \dot{v} does not change in the interval $[\bar{t}_1, \bar{t}_2]$, which implies there is only one switching between \bar{t}_0 and \bar{t}_2 . Proving that this does indeed occur is part of our ongoing future work.

Equations (12)–(14) yield $n + 2$ equations with $n + 2$ unknowns, $\gamma_0 = [x_0^T, \alpha_0]^T$, t_1 , and t_2 . We will refer to solving this set of simultaneous equations as the *limit cycle problem*. Due to the nonlinearity of these equations, we will utilize the well-known Newton-Raphson method to find a solution to the limit cycle problem. Denote our unknowns as $\Phi = [\gamma_0^T, t_1, t_2]^T$. We can then define

$$\mathcal{P}(\Phi) = \left[\Sigma^T(\Phi), H_1(\Phi), H_2(\Phi) \right]^T \quad (19)$$

We can now apply the Newton-Raphson method to obtain a solution to the above equation using the iterative formula

$$\Phi^{i+1} = \Phi^i - J^{-1}(\Phi^i) \mathcal{P}(\Phi^i) \quad (20)$$

where

$$J(\Phi) = \begin{bmatrix} \frac{\partial \Sigma}{\partial \gamma_0} & \frac{\partial \Sigma}{\partial t_1} & \frac{\partial \Sigma}{\partial t_2} \\ \frac{\partial H_1}{\partial \gamma_0} & \frac{\partial H_1}{\partial t_1} & \frac{\partial H_1}{\partial t_2} \\ \frac{\partial H_2}{\partial \gamma_0} & \frac{\partial H_2}{\partial t_1} & \frac{\partial H_2}{\partial t_2} \end{bmatrix}. \quad (21)$$

These partial derivatives can be readily calculated in closed-form based on (12)–(14); see the Appendix section for details. The limit cycle is then characterized by the solution of the equation

$$\mathcal{P}(\Phi^*) = 0. \quad (22)$$

Note that Φ^* completely characterizes the behavior of the limit cycles, as once the switching times and initial conditions are known, the closed-form solution of the limit cycle can be computed from successive solutions of the two (switching) linear systems. Note that the solution of (6) evolving according to Φ^* obeys the Poincare mapping

$$\gamma_0^* = \Psi(\gamma_0^*) \triangleq e^{A_1 t_2^*} e^{A_2 t_1^*} e^{A_1 t_2^*} e^{A_2 t_1^*} \gamma_0^*. \quad (23)$$

The (local) stability of this mapping is determined by linearizing the mapping about the fixed point γ_0^* ; if the eigenvalues have magnitude less than 1, then the solution is locally stable [14].

B. Properties of the Limit Cycles

While the solution of the limit cycle problem Φ^* must be calculated numerically, we can utilize the (12)–(14) to prove some properties of the limit cycles corresponding to the solution Φ^* . First, we will see how the solution Φ^* varies with the play radius r .

Proposition 1: Let the solution of the limit cycle problem with $r = r^*$ be denoted by $\Phi_{r^*} = [\gamma_0^{*T}, t_1^*, t_2^*]^T$. Then, if $r = r^* c_1$, where $c_1 > 0$, $\Phi_r = [c_1 \gamma_0^{*T}, t_1^*, t_2^*]^T$ is a solution to the limit cycle problem.

Proof: We begin by directly computing (13) evaluated at $\Phi_r = [c_1 \gamma_0^{*T}, t_1^*, t_2^*]^T$ with $r = r^* c_1$, which can be written as

$$[-K_1, 1][I - e^{A_1 t_1^*}]e^{A_2 t_1^*} c_1 \gamma_0^* = 2r^* c_1 \quad (24)$$

By dividing both sides by c_1 , we arrive at the solution of $H_2(\Phi_{r^*})$. Since the left-hand sides of (12) and (14) are linear with respect to the initial state, the c_1 term can be immediately divided out, proving $[c_1 \gamma_0^{*T}, t_1^*, t_2^*]^T$ solves the limit cycle problem. \square

Proposition 1 shows that there is a linear relationship between the play radius r and the amplitude of the limit cycles generated in (6), (7). Next, we can show that the bias of the limit cycles can be set to non-zero values. Consider the system

$$\begin{aligned} \dot{x}(t) &= Ax(t) + B(v(t) + W_r[v; 0](t)) \\ \dot{\sigma}(t) &= Cx(t) - y_r \\ v(t) &= -K_1 x(t) - K_2 \sigma(t) \end{aligned} \quad (25)$$

where y_r is a constant reference. The only difference between the above equation and our original system is the presence of the term y_r . Let us assume that

$$\text{rank} \begin{pmatrix} A & B \\ C & 0 \end{pmatrix} = n + 1$$

This is a well known necessary and sufficient condition for the existence of a steady-state solution to systems with constant references when integral control is used. Let $\bar{x} \in \mathbb{R}^n$ and $\bar{\sigma} \in \mathbb{R}$ be such that

$$0 = (A - BK_1)\bar{x} - BK_2\bar{\sigma}, \quad 0 = C\bar{x} - y_r. \quad (26)$$

Defining $\bar{v} = -K_1\bar{x} - K_2\bar{\sigma}$, we can see that (26) reduces to

$$\begin{bmatrix} A & B \\ C & 0 \end{bmatrix} \begin{bmatrix} \bar{x} \\ \bar{v} \end{bmatrix} = \begin{bmatrix} 0 \\ y_r \end{bmatrix}.$$

Therefore, our assumption guarantees the existence and uniqueness of \bar{x} and $\bar{\sigma}$. Next, define the coordinates

$$\tilde{x} = x - \bar{x}, \quad \tilde{\sigma} = \sigma - \bar{\sigma}. \quad (27)$$

Note that since y_r , \bar{x} and $\bar{\sigma}$ are constants, the closed-loop system can be written as [using (26)]

$$\begin{aligned} \dot{\tilde{x}}(t) &= (A - BK_1)\tilde{x}(t) + B(-K_2\tilde{\sigma}(t) + W_r[v; 0](t)) \\ \dot{\tilde{\sigma}}(t) &= C\tilde{x}. \end{aligned} \quad (28)$$

This is the same form as that considered in (1). Therefore, the system (25) and (7) possesses the same limit cycle as (6), (7), with the exception of a constant shift in the coordinates α and x . We present this result as the following proposition.

Proposition 2: Let $\Phi_0 = [\gamma_0^T, t_1, t_2]^T$ denote the solution of the limit cycle problem for (6), (7). Then, $\Phi^* = [(x_0 + \bar{x})^T, \alpha_0 - K_2\bar{\sigma}, t_1^*, t_2^*]^T$ is a solution to the limit cycle problem for the system (25) and (7).

Finally, we consider a special case of the system (1), where we assume x to be a scalar whose derivative obeys

$$\dot{x}(t) = ax(t) + (v(t) + W_r[v; 0](t))$$

where $a > 0$. We then select the control to be $v(t) = [k_p a, a^2/2]\gamma(t)$, where $k_p \in (0.5, 1)$. The eigenvalues of the systems then linearly scale with increasing a . The system matrices are then

$$\dot{\gamma}(t) = A_{i(t)}\gamma(t), \quad i = 1, 2 \quad (29)$$

where

$$A_1 = \begin{bmatrix} (1 - k_p)a & 1 \\ -a^2/2 & 0 \end{bmatrix}, \quad A_2 = \begin{bmatrix} (1 - k_p)a & 1 \\ -a^2 - k_p(1 - k_p)a^2 & -k_p a \end{bmatrix}.$$

We can now show that the frequency of the limit cycles is linearly related to the parameter a . Let us focus on the system in the boundary region of operation, i.e., $\dot{\gamma}(t) = A_2\gamma(t)$. The characteristic equation of this system is

$$s^2 - \text{Tr}(A_2)s + \text{Det}(A_2) = 0. \quad (30)$$

with

$$\text{Tr}(A_2) = (1 - 2k_p)a, \quad \text{Det}(A_2) = a^2$$

where Tr and Det denote the trace and determinant, respectively. Note that the condition $k_p \in (0.5, 1)$ implies, from the corresponding characteristic equations, that A_1 is unstable, and that A_2 is Hurwitz. Let us consider the state x as the output of this second-order system, and formulate a canonical form transformation. Let $\chi_1 = x$ and $\chi_2 = \dot{x}$. This transforms the system equations based on A_2 with our specified control gains into

$$\dot{\chi}_1(t) = \chi_2(t) \quad (31)$$

$$\dot{\chi}_2(t) = -a^2\chi_1(t) + (1 - 2k_p)a\chi_2(t). \quad (32)$$

Next, let $\eta_1 = a\chi_1$, and let $\eta_2 = \chi_2$. The $\dot{\eta}$ equations are then

$$\dot{\eta}_1(t) = a\eta_2(t) \quad (33)$$

$$\dot{\eta}_2(t) = -a\eta_1(t) + (1 - 2k_p)a\eta_2(t) \quad (34)$$

Finally, let the time variable $t = a\tau$, which implies that

$$\frac{d}{d\tau} = \frac{1}{a} \frac{d}{dt}.$$

Equation (33) now becomes

$$\frac{d\eta_1}{d\tau}(\tau) = \eta_2(\tau) \quad (35)$$

$$\frac{d\eta_2}{d\tau}(\tau) = -\eta_1(\tau) + (1 - 2k_p)\eta_2(\tau) \quad (36)$$

which is independent of a . The same transform can be applied to the system governed by the A_1 matrix, which then also becomes independent of a . The resulting system equations in these transformed coordinates are

$$\begin{aligned} \dot{\eta}(\tau) &= A_{\eta i}\eta(\tau), \quad i = 1, 2 \\ A_{\eta 1} &= \begin{bmatrix} 0 & 1 \\ -1/2 & (1 - k_p) \end{bmatrix}, \quad A_{\eta 2} = \begin{bmatrix} 0 & 1 \\ -1 & (1 - 2k_p) \end{bmatrix}. \end{aligned} \quad (37)$$

We can then apply (12)–(14) to (37), whose solution will be independent of a . By reversing the coordinate transforms on resulting solution,

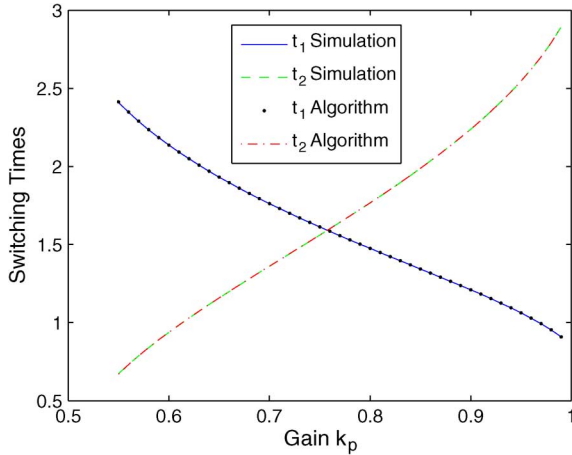


Fig. 3. Switching times computed from algorithm and simulation, versus gain k_p for the system described in (29).

we see that the effect of increasing a is to scale down the amplitude and scale up the frequency of the resulting oscillations. Equivalently, the switching intervals t_1 and t_2 are scaled by $1/a$. This result allows us to present the following proposition.

Proposition 3: Consider the system (29). Let the solution of the limit cycle problem with $a = a^*$ be denoted by $[\gamma_0^{*T}, t_1^*, t_2^*]^T$. Then, if $a = a^* c_1$, where $c_1 > 0$, $1/c_1 [\gamma_0^{*T}, t_1^*, t_2^*]^T$ is a solution to the limit-cycle problem.

III. SIMULATION RESULTS

We now continue our examination of the limit cycles through simulation. The first set of simulations are performed on a system obeying (29), where $a = 1$, and $r = 0.5$. First, we explore the variation of the solution to the limit cycle problem Φ^* with respect to the controller gain k_p . The effect of the gain k_p on the limit cycle solution is difficult to determine analytically; we instead explore its effect in simulation. Simultaneously, we verify the capability of the proposed Newton-Raphson method in computing the limit cycles by comparing its results to those observed in simulation.

Fig. 3 shows the switching times of the limit cycle as computed by both the Newton-Raphson algorithm and directly from simulation of the dynamics. The range of k_p considered was 0.55 to 0.99. There are several features of note on this figure. First, we are able to confirm the algorithm's effectiveness at computing the solution to the limit cycle with a scalar plant, as the simulation results agree very closely with the algorithm results. Second, looking at Fig. 3, we see that as k_p approaches 1, the system spends more and more time in the interior region (denoted t_2) versus the boundary region (denoted t_1). This is because the eigenvalues in the boundary region are significantly faster than those in the interior region when k_p is high, meaning the system must spend more time in the interior region to keep the system in steady state. Accordingly, smaller values of k_p results in the system spending more time in the boundary region than the interior region.

Fig. 4 shows the variation of the limit cycle solutions with k_p . Again, we see that the simulation and algorithm calculations are in tight agreement. Fig. 4 also indicates that as k_p approaches 0.5, the limit cycle solutions rapidly grow in size. This signals a rapid growth in the amplitude of the limit cycles for k_p , with the system becoming unstable for $k_p > 0.5$. Furthermore, Fig. 5 shows that the amplitude of the oscillations is strongly correlated with the size of α_0 .

We also verify the ability of our algorithm to predict solutions to limit cycles in higher order systems. We examine the limit cycles appearing in a system composed of a second-order plant, controlled by

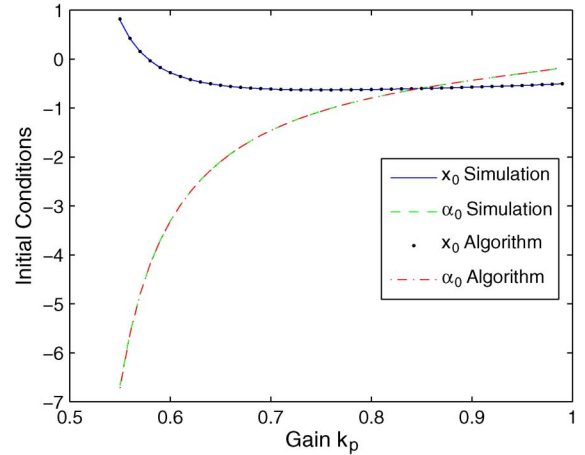


Fig. 4. Limit cycle solutions computed from algorithm and simulation, versus gain k_p for the system described in (29).

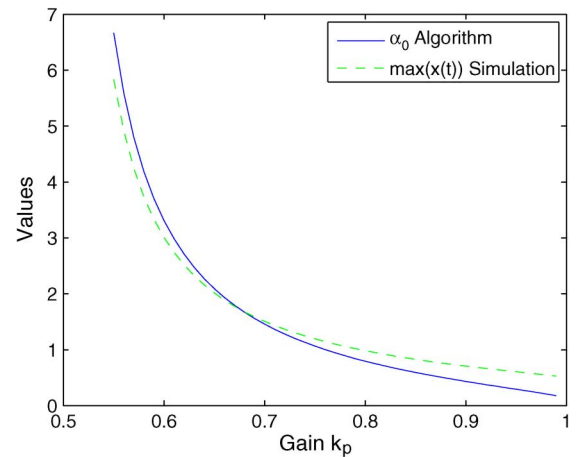


Fig. 5. Peak amplitude of limit cycles versus absolute value of the limit cycle solutions α_0 for the system described in (29).

a PI controller, and preceded by a unity gain and play operator. This system can be expressed in state-space form

$$\begin{aligned} \begin{bmatrix} \dot{x}_1(t) \\ \dot{x}_2(t) \end{bmatrix} &= \begin{bmatrix} 0 & 1 \\ -2 & 1 \end{bmatrix} \begin{bmatrix} x_1(t) \\ x_2(t) \end{bmatrix} + \begin{bmatrix} 0 \\ v(t) + W_r[v; 0](t) \end{bmatrix} \\ \dot{\sigma}(t) &= x_1(t) \\ v(t) &= k_p (-x_1(t) - 0.5x_2(t) - \sigma(t)) \end{aligned} \quad (38)$$

where $k_p = 1.8$. Figs. 6 and 7 show the evolutions of the initial state γ_0 and the switching times (t_1, t_2) , respectively, with the algorithm iterations. Observations of the convergence rates of different variables can be made from these figures. Around 60 iterations of our Newton-Raphson algorithm are required for the limit cycle solutions to settle to their final values, while the switching times converge significantly faster, requiring only around 20 iterations.

IV. CONCLUSIONS AND FUTURE WORK

We have demonstrated the ability to predict the properties of self-excited limit cycles generated by a system with hysteresis. Of particular interest is our result that the amplitude and periods of these limit cycles have linear relationships with the system parameters. We have also showed that a Newton-Raphson algorithm can be used to compute the closed-form of the limit cycles. These results can be utilized by control

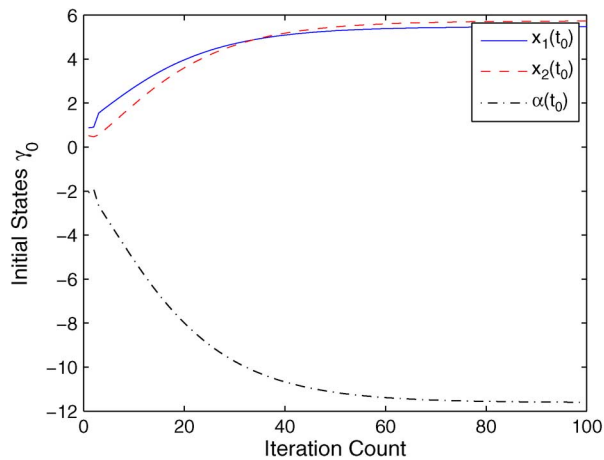


Fig. 6. Evolution of the limit cycle initial states, with successive Newton-Raphson iterations for the system described in (38).

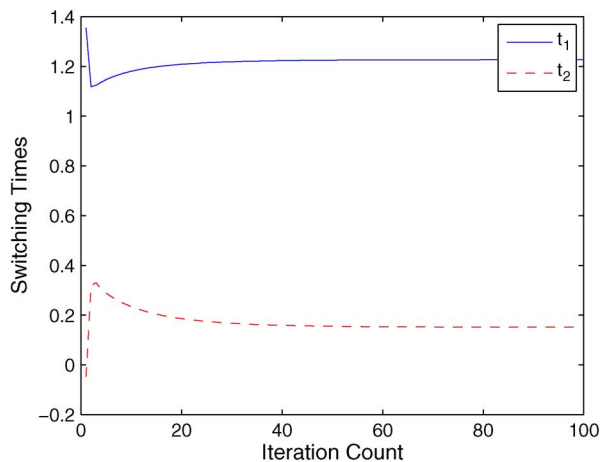


Fig. 7. Evolution of the switching times with successive Newton-Raphson iterations for the system described in (38).

designers to alter control designs to either create or eliminate oscillations in systems with backlash. Future work will include investigating whether (22) admits a unique solution, as our computational examples have suggested. We will also explore the extension of this work to PI operators with multiple play hysterons, where a significant challenge arises from the much larger number of possible switches in the dynamics.

REFERENCES

- [1] S. Devasia, E. Eleftheriou, and S. O. R. Moheimani, "A survey of control issues in nanopositioning," *IEEE Trans. Control Syst. Technol.*, vol. 15, pp. 802–823, 2007.
- [2] S. Bashash and N. Jalili, "Robust adaptive control of coupled parallel piezo-flexural nanopositioning stages," *IEEE/ASME Trans. Mechatron.*, vol. 14, pp. 11–20, Nov. 2009.
- [3] P. Ge and M. Jouaneh, "Tracking control of a piezoceramic actuator," *IEEE Trans. Control Syst. Technol.*, vol. 4, no. 3, pp. 209–216, 1996.
- [4] G. Tao and P. V. Kokotovic, "Adaptive control of plants with unknown hystereses," *IEEE Trans. Autom. Control*, vol. 40, no. 2, pp. 200–212, Feb. 1995.
- [5] J. W. Macki, P. Nistri, and P. Zecca, "Periodic oscillations in systems with hysteresis," *Rocky Mountain J. Math.*, vol. 22, no. 2, 1992.
- [6] A. Cavallo, C. Natale, S. Pirozzi, and C. Visone, "Limit cycles in control systems employing smart actuators with hysteresis," *IEEE/ASME Trans. Mechatron.*, vol. 10, no. 2, pp. 172–180, Apr. 2005.

- [7] A. Mees and A. Bergen, "Describing functions revisited," *IEEE Trans. Autom. Control*, vol. AC-20, no. 4, pp. 473–478, Aug. 1975.
- [8] A. Bergen, L. Chua, A. Mees, and E. Szeto, "Error bounds for general describing function problems," *IEEE Trans. Circuits Syst.*, vol. CAS-29, no. 6, pp. 345–354, Jun. 1982.
- [9] I. Babaa, T. Wilson, and Y. Yu, "Analytic solutions of limit cycles in a feedback-regulated converter system with hysteresis," *IEEE Trans. Autom. Control*, vol. AC-13, no. 5, pp. 524–531, Oct. 1968.
- [10] M. Krasnoselskii and A. Pokrovskii, *Systems With Hysteresis*. Berlin-Heidelberg-New York-Paris-Tokyo: Springer-Verlag, 1989.
- [11] P. Krejci, "Hysteresis and periodic solutions of semilinear and quasilinear wave equations," *Mat. Zeit.*, no. 193, pp. 247–264, 1986.
- [12] A. J. Ijspeert, "Central pattern generators for locomotion control in animals and robots: A review," *Neural Netw.*, vol. 21, pp. 642–653, 2008.
- [13] X. Tan and H. K. Khalil, "Two-time-scale averaging of systems involving operators and its application to adaptive control of hysteretic systems," in *Proc. 2009 Amer. Control Conf.*, 2009, pp. 4476–4481.
- [14] A. Girard, "Computation and stability analysis of limit cycles in piecewise linear hybrid systems," in *Proc. 1st IFAC Conf. Analysis and Design of Hybrid Systems*, 2003, pp. 181–186.

Particle Filtering Framework for a Class of Randomized Optimization Algorithms

Enlu Zhou, Michael C. Fu, and Steven I. Marcus

Abstract—We reformulate a deterministic optimization problem as a filtering problem, where the goal is to compute the conditional distribution of the unobserved state given the observation history. We prove that in our formulation the conditional distribution converges asymptotically to a degenerate distribution concentrated on the global optimum. Hence, the goal of searching for the global optimum can be achieved by computing the conditional distribution. Since this computation is often analytically intractable, we approximate it by particle filtering, a class of sequential Monte Carlo methods for filtering, which has proven convergence in "tracking" the conditional distribution. The resultant algorithmic framework unifies some randomized optimization algorithms and provides new insights into their connection.

Index Terms—Cross-entropy method, particle filtering, randomized optimization.

I. INTRODUCTION

Global optimization problems arise in many areas of importance and can be extremely difficult to solve, due to the presence of multiple local optimal solutions and the lack of structural properties such as differentiability and convexity. In a general setting, there is little problem-specific knowledge that can be exploited in searching for improved solutions, and it is often the case that the objective function can only be

Manuscript received April 01, 2012; revised December 13, 2012; accepted August 20, 2013. Date of publication September 09, 2013; date of current version March 20, 2014. This work was supported in part by the National Science Foundation (NSF) under Grants CNS-0926194, CMMI-0856256, EEC-0901543, CMMI-1130273, and by the Air Force Office of Scientific Research (AFOSR) under Grant FA9550-10-1-0340. Recommended by Associate Editor L. H. Lee.

E. Zhou is with the H. Milton Stewart School of Industrial and Systems Engineering, Georgia Institute of Technology, GA 30332 USA (e-mail: enlu.zhou@isye.gatech.edu).

M. C. Fu and S. I. Marcus are with the Institute for Systems Research, University of Maryland, College Park, MD 20742 USA (e-mail: mfu@umd.edu; marcus@umd.edu).

Digital Object Identifier 10.1109/TAC.2013.2281132